

Inherent nature of localized states in highly planar monolayer InAs/GaAsN pseudo-alloys

I. L. Krestnikov,^{a),b)} R. Heitz, N. N. Ledentsov,^{a)} and A. Hoffmann

Institut für Festkörperphysik, Technische Universität Berlin, Hardenbergstrasse 36, 10623, Berlin, Germany

A. M. Mintairov, T. H. Kosel, and J. L. Merz

Department of Electrical Engineering, University of Notre Dame, Notre Dame, Indiana

I. P. Soshnikov and V. M. Ustinov

A. F. Ioffe Physical-Technical Institute of Russian Academy of Sciences, Politekhnicheskaya 26, 194021, St. Petersburg, Russia

(Received 20 June 2003; accepted 5 September 2003)

We have studied the optical properties of pseudo-alloy monolayer InAs/GaAsN superlattices with highly planar interfaces. In spite of the two-dimensional growth mode, we found that the photoluminescence (PL) reveals strong exciton localization through the whole PL band, dominating the spectrum up to high excitation densities and observation temperatures. Pump-and-probe PL experiments provide the following time constants: (a) the exciton relaxation time to the ground states of the localization regions is found to be $\sim 40\text{--}70$ ps, depending on the photon energy, and (b) the time for depopulation of these localized states is between 2 and 4 ns. © 2003 American Institute of Physics. [DOI: 10.1063/1.1623320]

Group III arsenide nitrides provide a unique opportunity for bandgap engineering,^{1–3} and for the modification of the optical and electrical properties of the media that are important for numerous device applications. The large lattice mismatch between GaAsN and GaAs can be alleviated by the incorporation of indium to form the quaternary InGaAsN. Recently, lasing in the $1.3\ \mu\text{m}$ range on GaAs substrates^{4–6} was achieved, and the possibility of injection lasing in the $1.5\ \mu\text{m}$ spectral range was demonstrated.⁷ At the same time, there exists a controversy in understanding the optical and electric properties of InGaAsN-GaAs structures. It was found that high indium content InGaAsN layers on a GaAs substrate demonstrate a clear tendency towards surface and interface corrugation, which may lead to spontaneous formation of three-dimensional (3D)-like islands.⁸ Such 3D structures can be viewed as semiconductor quantum dots (QDs).⁹ Thus, the photoluminescence (PL) properties of such structures may represent those of InAs-GaAs quantum dots rather than that of an “intrinsic” InGaAsN layers. Several approaches have been proposed to suppress the effect of surface corrugation, for example, Sb doping.¹⁰ However, it was also found that even in the case of planar interfaces, small changes in the N composition lead to the formation of localized states,¹¹ and this effect was observed regardless of the presence or absence of In.¹²

In this letter, we study InAs/GaAsN monolayer superlattices (SLs) with highly planar interfaces and an average lattice parameter approximately equal to the lattice parameter of the GaAs substrate to ensure the absence of 3D InGaAsN domains, which could affect the optical properties of the material. With respect to the ultrashort periodicity, these SLs should behave as pseudo-alloy layers with little impact of the

finite minizone width on electron and hole transport properties. In spite of this fact, we report results of PL, PL excitation (PLE), and time-resolved (TR) PL studies, which demonstrate the extreme role of localized states up to high excitation densities and temperatures. These results are consistent with the results of near-field magnetoluminescence measurements of single QDs in this sample reported earlier,¹¹ and they prove the basic nature of exciton localization even in lattice-matched InGaAsN pseudo-alloys.

The sample studied in this work was grown by molecular-beam epitaxy on GaAs(001) substrates at $T=450\text{ }^\circ\text{C}$. A rf plasma source was used to generate atomic nitrogen from N_2 . A 40-period InAs/GaAs_{1–y}N_y ($y=0.034$) SL was grown with InAs and GaAs_{1–y}N_y layer thicknesses of 0.25 and 2.82 nm, respectively, representing a pseudo-alloy with average In and N concentrations of 0.08 and 0.03, respectively, and an average composition lattice matched to the GaAs substrate. This pseudo-alloy layer was sandwiched between AlGaAs layers of thickness 60 (bottom) and 14 (top) nm. The structure was capped by a 20 nm GaAs layer and annealed at $730\text{ }^\circ\text{C}$ for 10 min. Transmission electron microscope (TEM) images were taken at 100 kV in a Philips CM30 microscope. Bright-field conditions and 004-electron reflection were used for the TEM imaging. The PLE spectra were excited with the monochromatized light from a tungsten lamp. For pump-and-probe measurements and TRPL investigations a solid-state tunable infrared laser (Opal Spectra-Physics), pumped by a Ti-sapphire mode-locked laser, was used. The wavelength for the pump and probe beams was chosen as 1083 nm. The average powers of the pump and probe beams were 30 and 3 mW, respectively. The pump and probe beams were focused to a spot size of about $70\ \mu\text{m}$ at the same area of the sample. An optical delay was inserted in the pump beam, which allowed changing the optical delay of the pump and probe pulses with an accuracy better than 1

^{a)}On leave from Ioffe Institute.

^{b)}Electronic mail: igor@sol.physik.tu-berlin.de

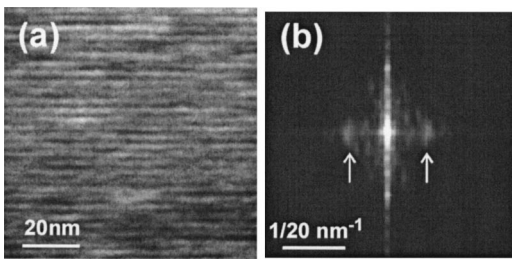


FIG. 1. (a) 004 bright-field TEM image of the structure. (b) 2D Fourier transformation of the TEM image.

ps. The probe beam was mechanically modulated with a frequency of 200 Hz and the PL signal was detected with a lock-in system using an InGaAs photodiode. In this case the PL signal from the probe beam could stand out against a background of the PL signal from the pump beam. TRPL data were obtained using a fast multichannel photomultiplier.

Figure 1(a) shows a cross-section TEM image of the sample, evidencing the well-pronounced highly planar SL in the vertical direction, with additional contrast perpendicular to the growth direction because of weaker compositional modulation in the lateral direction. This additional contrast can be attributed to lateral regions with different indium and/or nitrogen concentration. To evaluate the characteristic lateral size, we applied a two-dimensional (2D) Fourier transformation to the TEM image [Fig. 1(b)]. In addition to a zero spot due to long-wavelength disorder, one can resolve two streaks (marked by arrows) corresponding to the lateral quasiperiodicity. Clearly resolved sharp spots due to the vertical periodicity were also observed, but not shown in Fig. 1(b) as they are much farther away from the zero spot. The relative separation of the streaks amounts to 8 nm, a value that is in good agreement with the lateral extension of the localized exciton radii estimated in Ref. 11 by magneto-PL.

In Fig. 2(a), we show PL (thick lines) and PLE spectra measured at low temperature. The PL registration energies (i.e., detection energies) for the PLE spectra are indicated by arrows at 1.105, 1.083, 1.063, and 1.023 eV. At low excitation density (<100 mW/cm²), the PL spectrum is dominated by the peak at 1.08 eV. The intensity of this emission saturates with an increase of the excitation density and the PL peak at 1.102 eV becomes dominant. This PL peak does not shift to higher photon energies with increasing excitation density (up to high pump levels of a few kW/cm²). With increasing temperature, the photon energy of this peak [Fig. 2(b), solid squares] follows the GaAs bandgap temperature dependence [Fig. 2(b), dotted line]. Conversely, the peak (1.08 eV at low temperature) dominating the spectrum at low excitation densities exhibits a so-called “S-shape” behavior with increasing temperature [Fig. 2(b), open circles]. The fact that the PL line at 1.102 eV does not shift to higher energies with higher excitation density and follows the GaAs bandgap temperature dependence indicates that it corresponds to the maximum in the density of radiative states in the system.

Surprisingly, the onset energy of the PLE spectrum (1.15 eV) is strongly shifted from the maximum of the PL (1.102 eV) spectrum (by ~ 50 meV). This behavior is not expected for quantum well samples, in which such a Stokes shift may exist only in case of emission from the low-energy localized

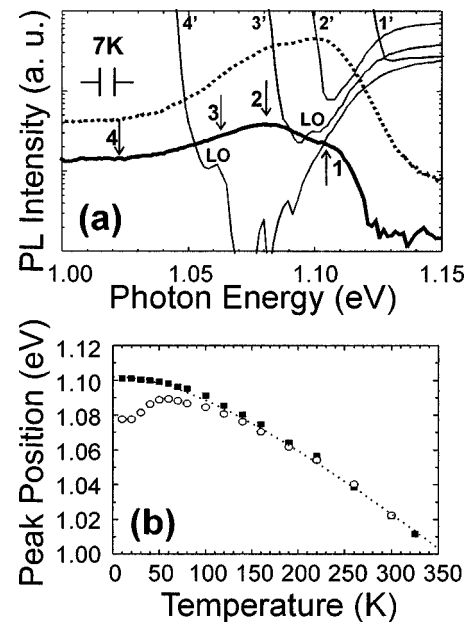


FIG. 2. (a) Spectra of PL (thick line) and PLE (thin lines) measured at excitation density of 3 mW/cm². Registration energies (i.e., detection energies) for PLE spectra are (1) 1.105, (2) 1.083, (3) 1.063, and (4) 1.023 eV, marked by arrows. Thick dotted line corresponds to the PL spectrum measured at excitation density of 10 W/cm². (b) Temperature dependencies of maximum of PL spectra measured at excitation densities of 10 W/cm² (solid squares) and 50 mW/cm² (open circles). The dotted line represents a calculation of the temperature dependence of the GaAs bandgap using Varshni's expression.

states, and is not possible for luminescence originating from the maximum in the density of states. Conversely, such an observation is typical for QD structures, in which the PLE onset is strongly shifted towards the high-energy side of the spectrum with respect to the PL maximum.¹³ The effect of the PLE onset displacement originates due to the delta-function-like absorption spectrum of quasi-ideal QDs and the lack of energy transfer between the size dispersed QDs at low temperatures. In this case, the population of QDs having a fixed ground state energy is possible either resonantly with the ground states, or with the well-separated excited or continuum states, causing a characteristic onset shift in the PLE spectra.¹³ One may assume, therefore, that the PLE onset originates from the mobility edge of the InGaAsN pseudo-alloy layer.

Key information concerning exciton trapping and the population of localized states in the pseudo-alloy layer can be obtained from pump-and-probe PL studies. In this experiment, one varies the delay time between the pump and the probe pulses and detects PL at different registration energies only from the probe beam due to lock-in system. Figure 3(a) shows the PL intensity as a function of delay time. The PL signals are normalized with respect to the PL intensity without the pump beam, and are offset in the figure for clarity. In the case of delay times longer than ~ 300 ps the PL signal due to the probe beam is significantly reduced, as compared to the signal without the pump excitation. This occurs because the localization centers are already partly filled by the pump pulse, so that the probe pulse cannot populate all of these states. The signal restores its value with further increase in the delay time indicating weaker impact of the pump pulse. In the course of time the carriers generated by

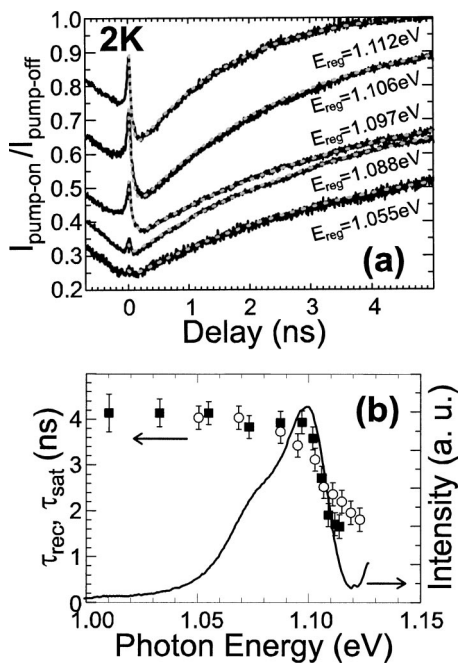


FIG. 3. (a) Normalized pump-and-probe PL intensity versus delay time between pump-and-probe pulses measured at different registration energies. Dotted gray lines are a fitting from Eq. (1). (b) Dependence of recombination time (τ_{rec}) and saturation time (τ_{sat}) versus registration energy, showing that they are essentially identical. Solid squares obtained from pump-and-probe experiments and open circles are from TRPL experiments. A time-integrated PL spectrum is presented by solid lines.

the pump pulse depopulate localized states and the “probe” signal pulse increases with a characteristic time τ_{sat} . In our experimental setup the maximum delay between the pump and the probe pulses (6.25 ns) is sufficient to cause the depopulation of most of the states, and hence full recovery of the probe-induced luminescence. However, slow components at the low energy side of the PL spectrum retain a small, but measurable population, causing signal saturation at values somewhat below unity. The drop of the PL signal for negative delay time between the pump and the probe pulses has the same nature. In this technique, accurate measurements of the time scale are of utmost importance, making it possible to determine the origin of the depopulation process through the whole band of localized states.

The pump-probe technique provides additional information concerning the nature of the localized states and the dynamics of the recombination process, as the carriers generated by the pump pulse need a finite time to relax into particular localized states. There exists, therefore, a period near zero delay time when the probe signal luminescence is still strong. If the localized state is not yet filled by carriers generated by the pump pulse, the carriers generated by the probe pulse can still compete and occupy this particular state, giving rise to probe-signal PL. These phenomena allow us to evaluate both the pump relaxation time constant (τ_{rel}) and the probe signal saturation time constant (τ_{sat}) by fitting the experimental curves with the following equation:

$$I \sim 1 - \{1 - \exp(-t/\tau_{rel})\} \exp(-t/\tau_{sat}). \quad (1)$$

The results of the fitting are shown in Fig. 3(a) by dotted gray lines. The estimated relaxation time is about 40 ps for

localized states on the high-energy side of the PL peak and up to 70 ps at the low-energy side of the PL. The saturation time constants are presented in Fig. 3(b) by solid squares, while the open circles represent the decay times (recombination time τ_{rec}) obtained from TRPL. As follows from the comparison of TRPL and pump-and-probe studies, the major mechanism for carrier depopulation through the whole PL band is radiative recombination. No signs of ultrafast depopulation of the states even on the high-energy side of PL emission were found. This observation clearly confirms our suggestion concerning the effective carrier localization and the lack of carrier transport between the localized states derived from comparison of PL, PLE, and temperature-dependent PL data. Conversely, for quantum wells or for conventional alloy layers, such a behavior in population and depopulation processes within the localized band states is completely unusual.¹⁴

In conclusion, our results demonstrate exciton localization in InGaAsN pseudo-alloys through the entire luminescence band originating from fundamental bandgap transitions. The intrinsic nature of the localization is demonstrated in PL, PLE, temperature-dependent PL, and TRPL, consistent with the results of magneto-PL.¹¹ Additionally, pump-and-probe PL studies allow one to define, independently, the carrier capture time and the depopulation time for the localized states studied. The decay time is governed by radiative recombination of the localized excitons through the whole PL band and the time constants are close to those reported for InAs/GaAs QDs.

This work was supported by the DFG Graduiertenkolleg “Collective phenomena in solids,” the RFBR and the grant “NATO Science for Peace.” One of the authors (I.L.K.) thanks the Alexander von Humboldt Foundation. Another author (N.N.L.) acknowledges a DAAD Guest Professorship and equipment donation from the Alexander von Humboldt Foundation. A third (J.L.M.) thanks the Alexander von Humboldt Foundation for a Research Award, and the Paul Drude Institute for a Guest Professorship. The authors also thank R. E. Cook, Argonne National Laboratory, for the TEM image.

¹P. R. C. Kent and A. Zunger, Phys. Rev. Lett. **86**, 2613 (2001).

²S. Sakai, Y. Ueta, and Y. Terauchi, Jpn. J. Appl. Phys. **32**, 4412 (1993).

³S.-H. Wei and A. Zunger, Phys. Rev. Lett. **76**, 664 (1996).

⁴K. Nakahara, M. Kondow, T. Kitatani, M. C. Larson, and K. Uomi, IEEE Photonics Technol. Lett. **10**, 487 (1998).

⁵A. Yu. Egorov, D. Bernklau, D. Livshits, V. M. Ustinov, Zh. I. Alferov, and H. Riechert, Electron. Lett. **35**, 1643 (1999).

⁶G. Steinle, H. Riechert, and A. Yu. Egorov, Electron. Lett. **37**, 93 (2001).

⁷M. Fischer, M. Reinhardt, and A. Forchel, Electron. Lett. **36**, 1208 (2000).

⁸B. V. Volovik, A. R. Kovsh, W. Passenberg, H. Kuenzel, N. Grote, N. A. Cherkashin, Yu. G. Musikhin, N. N. Ledentsov, D. Bimberg, and V. M. Ustinov, Semicond. Sci. Technol. **16**, 186 (2001).

⁹M. Sopian, H. P. Xin, and C. W. Tu, Appl. Phys. Lett. **76**, 994 (2000).

¹⁰J. C. Harmand, G. Ungaro, L. Largeau, and G. Le Roux, Appl. Phys. Lett. **77**, 2482 (2000).

¹¹A. M. Mintairov, J. L. Merz, T. Kosel, P. Blagnov, A. S. Vlasov, V. M. Ustinov, and R. E. Cook, Phys. Rev. Lett. **87**, 277401 (2001).

¹²A. M. Mintairov and J. L. Merz (unpublished).

¹³N. N. Ledentsov, M. Grundmann, N. Kirstaedter, O. Schmidt, R. Heitz, J. Böhrer, D. Bimberg, V. M. Ustinov, V. A. Shchukin, P. S. Kop'ev, Zh. I. Alferov, S. S. Ruvimov, A. O. Kosogov, P. Werner, U. Richter, U. Gösele, and J. Heydenreich, Solid-State Electron. **40**, 785 (1996).

¹⁴C. Gourdon and P. Lavallard, Phys. Status Solidi B **153**, 641 (1989).